Spin-Dependent Hot Electron Transport in Co/Cu Thin Films

W. H. Rippard and R. A. Buhrman
School of Applied and Engineering Physics, Cornell University, Ithaca, New York 14853
(Received 31 August 1999)

Hot-electron transport in Co/Cu/Co trilayer films has been studied in the energy range from 1.0 to 2.0 eV using ballistic electron magnetic microscopy. Both the spin-dependent attenuation lengths of Co and the cumulative polarizing effects of spin-dependent tunneling and transmission across a Co/Cu interface have been determined. For very thin (a few Å) Co layers, the latter effects result in a weakly majority-spin polarized electron beam above ~1.3 eV and a minority-spin polarized beam below ~1.2 eV. For thicker Co layers the transmitted beam is always majority-spin polarized.

PACS numbers: 73.23.Ad, 73.40.–c, 75.70.–i

The spin-dependent electron scattering behavior of thin ferromagnetic films, and the spin-filtering effects of transport across ferromagnetic/nonferromagnetic metal interfaces are fundamental to the understanding and application of the magnetotransport properties of magnetic multilayer systems. These have important implications for both the flow of electrons with energies at the Fermi level, i.e., the giant magnetoresistance effect, and for hot-electron devices and transport phenomena [1,2]. In recent years there have been a number of efforts to establish the spin-dependent transport properties of ferromagnetic layers in the hot electron regime. These studies [3,4] have typically used spin-polarized photoemission and the measurement of the attenuation of spin-polarized beams when passed through a magnetic layer. Consequently the measurements have been made using electrons with energies much greater than 1 eV, and hence at energies well above the minority electron *d*-band and above the most appropriate energy scale for devices based on the combination of ferromagnetic and semiconductor materials. While there has been an important study [5] of the spin-dependent quasiparticle lifetimes in a ferromagnet (Co) at energies ~1 eV and below, there has yet to be any precise measurement of either the spin-dependent attenuation lengths or the spin-dependent transmission probabilities of ferromagnet/normal-metal interfaces in this energy range.

Here we report on measurements probing spin-dependent hot-electron transport utilizing scanning tunneling microscopy (STM) and a new technique for imaging magnetic domain structure in thin film multilayers. This technique, ballistic electron magnetic microscopy (BEMM) [6], allows us to establish the relative magnetic orientation of Co/Cu/Co thin film trilayers during the measurements and to monitor their change from ferromagnetic (F) to antiferromagnetic (AF) alignment under application of a magnetic field H. From hot (1–2 eV) electron transmission measurements taken as a function of Co layer thickness and relative magnetic alignment, we obtain, to good precision, both the spin-dependent attenuation lengths of thin Co films and the energy dependence of the relative transmission factors for tunnel-injected majority and minority electrons across a Co/Cu interface.

In BEMM, a variation of ballistic electron emission microscopy (BEEM) [7,8], multiple thin ferromagnetic films separated by nonferromagnetic spacer layers are grown on a semiconductor substrate. An STM tip is then used to locally inject current I_t into the multilayer film under normal constant-current feedback conditions. Once in the film, some fraction of the injected electrons (typically $<10\%$) will travel ballistically through the film and underlying metal-semiconductor interface. The current flowing into the semiconductor (the collector current I_c) is then measured and displayed as a function of the position of the tip, creating a BEMM image, e.g., Fig. 1, which is a spatial map of ballistic electron transport through the multilayer film. Contrast in these images is due to the relative magnetization alignment between the ferromagnetic films. When the local magnetization directions are antiparallel, I_c is a minimum, whereas when the magnetization directions are aligned, I_c is a maximum. Typical BEMM images from a Co/Cu/Co trilayer film taken with a nonmagnetic, etched W tip, at a fixed position with H applied parallel to the film plane are shown in Figs. 1(a) and 1(b). The images show the magnetic structure of the film in (a) the as-prepared state with no field having been applied and (b) the state of saturated magnetization in H = 60 Oe.

The samples used in this investigation consist of both Co/Cu/Co trilayer films and single Co layer films grown at ~300 K on a Si(111) H-terminated substrate precoated with a thin Cu/Au bilayer, to form a high-quality Au/Si Schottky barrier interface, and a Cu seed layer for the Co growth. For the single Co layer samples, this bilayer is ~75 Å Au(111) and ~45 Å Cu(111) [9] on top of which a Co(111) layer of varying thickness is grown. The trilayer films are grown on a Au (75 Å)/Cu (9 Å) bilayer and the two Co layers are separated by a 45 Å Cu spacer layer which leaves them only weakly coupled by indirect exchange [10]. The total Au and Cu thicknesses of the different samples are always the same to within 10 Å and thus can be considered identical due to the long inelastic scattering lengths (~200 Å) of noble metal films [9].

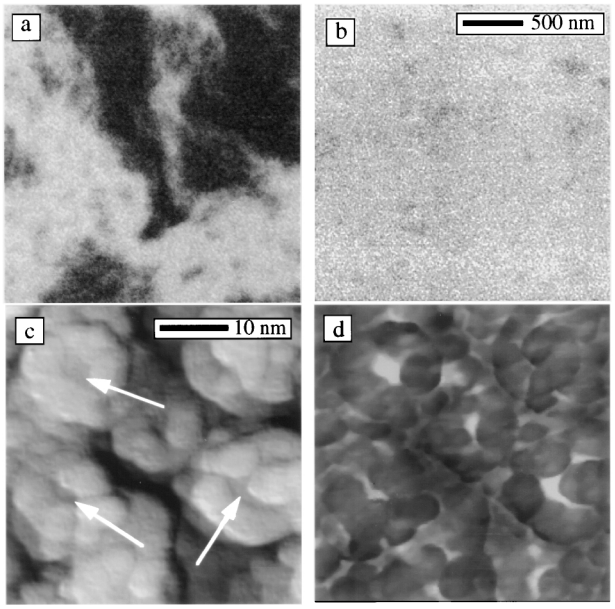

FIG. 1. (a),(b) BEMM ($2.5 \times 2.5\ \mu m^2$) images taken at a fixed position in a varying magnetic field (a) before field applied and (b) applied field of 60 Oe. The sample is Co (30 Å)/Cu (45 Å)/Co (30 Å)/Cu (9 Å)/Au (75 Å). I_c is represented in a linear gray scale with a range from 0.5 pA (black) to 2.5 pA (white). $V_t = -1.5$ V and $I_t = 5$ nA. The (c) height (gray scale of 2 nm) and (d) BEEM image (black = 3 pA, white = 12.5 pA) of a Co (~3 Å)/Cu (30 Å)/Au (100 Å) film; the Co film is discontinuous. Arrows indicate examples of exposed regions of Cu. I_c through exposed Cu regions is 10 pA on average and through the Co covered regions is 5 pA on average. $V_t = -1.2$ V and $I_t = 2$ nA.

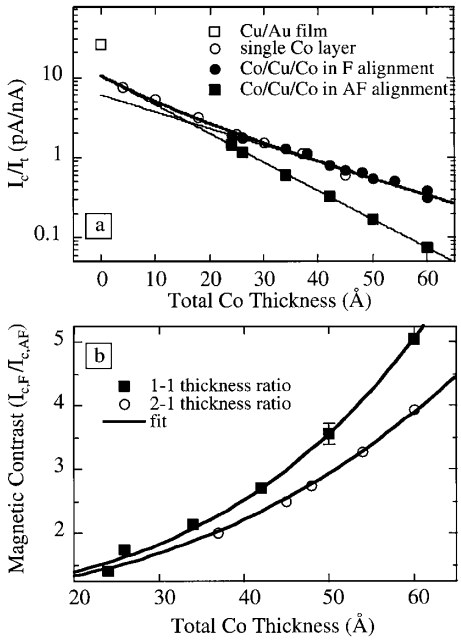

FIG. 2. (a) I_c/I_t for Co single layer and Co/Cu/Co trilayer films as a function of total Co thickness and for a Cu/Au film (uncertainty in I_c is ±5%). The total Cu and Au layer thicknesses are approximately the same for all samples. Currents from trilayer films are taken in regions of both F alignment and AF alignment. $V_t = -1.5$ V. (b) The magnetic contrast $I_{c,F}/I_{c,AF}$ for Co/Cu/Co films as a function of total Co thickness. $V_t = -1.5$ V.

The films are thermally evaporated in ultrahigh vacuum (UHV) with the pressure remaining $< 5 \times 10^{-10}$ Torr during deposition and then vacuum transferred into a room-temperature UHV BEMM chamber for study.

Figure 2(a) shows the values of I_c as a function of total Co thickness for both single (○) and trilayer samples, as averaged over many different regions of each sample with a tip bias $V_t = -1.5$ V. In the case of the Co/Cu/Co trilayer films the regions over which the averages are taken correspond to either regions of F or AF alignment. The data from regions of F alignment (●) are from trilayer films with either a 1:1 or 2:1 Co layer thickness ratio, while the data from regions of AF alignment (■) are shown here only for films with a 1:1 thickness ratio, for reasons discussed below.

The data from the single layer samples and trilayer samples in F alignment extrapolate to zero Co thickness well below the measured current through a single Cu/Au film of the same thickness. This large reduction of the ballistic electron beam is due to the band-structure mismatch at the Co/Cu interface [11]; an effect which is enhanced by the strongly forward-focused momentum distribution of tunnel-injected electrons. At the energies used here, Cu(111) has no propagating momentum states in the directions lying in a large cone about the film normal, a cone much larger than for Co(111). Thus, while the electrons from the STM tip tunnel preferentially to states of relatively small transverse momentum in the Co, many of these have no matching states in the Cu in which to propagate. Because of conservation of momentum parallel to the interface, a large fraction of the tunnel-injected electrons are reflected at the Co/Cu interface. The strength of this momentum filtering effect is determined by the relative sizes of the Fermi surfaces of Co and Cu and so is stronger for the minority than for the majority electrons [11].

This filtering effect of the Co/Cu interface is demonstrated directly in Figs. 1(c) and 1(d), where a discontinuous layer of Co has been deposited on a Cu/Au film. A Cu/Au film grown on a Si(111) substrate consists of grains ~15 nm in diameter, whose top surfaces are typically atomically flat but occasionally transected by an atomic step. As shown in the STM and BEEM images, when ~2–3 Å of Co is evaporated on top of these films, the Co atoms migrate preferentially to grain boundaries and steps on the surface where they coalesce to form small grains ~5 nm in diameter and ~4–5 Å high. Arrows in Fig. 1(c) show examples of still uncovered Cu surfaces, where I_c, as shown in Fig. 1(d), is approximately a factor of 2 higher than when the electrons pass through just two atomic layers of Co. As indicated by Fig. 2(a), this difference is much too great to be accounted for by the attenuation length of the Co and so must be largely due to scattering (reflection) at the Co/Cu interface.

While the tunnel-injected electron beam is strongly reduced upon passing through a single Co(111)/Cu(111) interface, the presence of a second interface has little effect on the ballistic electrons whose momentum distribution has been filtered by the first interface. This is demonstrated in Fig. 2(a) by the Co/Cu/Co samples in F alignment, where I_c is within a few percent of the value measured for a single Co layer of the same thickness. This, in turn, establishes that there is no substantial elastic scattering of the momentum-filtered hot electrons emerging from the first Co layer in passing through the intervening Cu spacer layer.

The following equations [12] are used to describe the collector current for F and AF alignment of the trilayer films in the case where the Co layers have the same thickness:

$$I_{c,\mathrm{F}} = I_o[\, f_\uparrow T_{o\uparrow} T^*_{i\uparrow} T^*_{o\uparrow} \exp(-2w/\lambda_\uparrow) + f_\downarrow T_{o\downarrow} T^*_{i\downarrow} T^*_{o\downarrow} \exp(-2w/\lambda_\downarrow)\,], \quad (1)$$

$$I_{c,\mathrm{AF}} = I_o[\, f_\uparrow T_{o\uparrow} T^*_{i\downarrow} T^*_{o\downarrow} \exp(-w/\lambda_+) + f_\downarrow T_{o\downarrow} T^*_{i\uparrow} T^*_{o\uparrow} \exp(-w/\lambda_+)\,]. \quad (2)$$

(The analogous equations for single Co layer films and for trilayer films where the Co layers are of different thicknesses are straightforward and so are not given here.) Here I_o is an overall scaling factor, $f_{\uparrow(\downarrow)}$ is the fraction of majority (minority) electrons in the initial tunnel current injected into the top Co layer due to a spin-dependent density of states (DOS) in Co [13], $\lambda_{\uparrow(\downarrow)}$ is the majority (minority) attenuation length, $T_{o(i)\uparrow(\downarrow)}$ is the transmission coefficient for majority (minority) electrons out of (into) a Co layer, w is the thickness of an individual Co layer, $1/\lambda_+ = 1/\lambda_\uparrow + 1/\lambda_\downarrow$, and the $*$ denotes that the Co layer is buried underneath the Cu spacer layer. The distinction between the transmission coefficients for the first and second Co layers must be made since, as noted above, the momentum distribution of the electrons entering the second layer has been previously filtered by the first Co/Cu interface.

The $I_{c,\mathrm{F}}$ data in Fig. 2(a) can be fit directly with Eq. (1), but such a four-parameter fit to the data leads to a large uncertainty as to the uniqueness of the results. We reduce the number of free parameters in this fit and demonstrate the accuracy of the fitted results, by using the imaging capabilities of BEMM to determine I_c as a function of magnetic alignment between the Co films as well as of film thickness. We first analyze the $I_{c,\mathrm{AF}}$ data taken as a function of Co thickness, shown as (■) in Fig. 2(a). These data are fit directly with Eq. (2), which has only two free parameters, λ_+ and a single preexponential term (using a 1:1 Co thickness ratio in the trilayers reduces the number of independent parameters in the fit from 4 to 2). A fit to the data gives $\lambda_+ = 6.0 \pm 0.5$ Å. Next we analyze the I_c data from the single Co layer films and $I_{c,\mathrm{F}}$ from the trilayer films, using only thick (>40 Å) films where the variation of the current clearly follows a simple exponential decay. This allows the data to be fit with two parameters, a preexponential term and $\lambda_\uparrow$ (assumed to be the longer of the two attenuation lengths) [3,4], yielding $\lambda_\uparrow = 21 \pm 1$ Å. By then taking the ratio of the $w = 0$ intercepts, shown in Fig. 2(a), of the single-exponential functions that are fit, respectively, to the $I_{c,\mathrm{AF}}$ data and to the $I_{c,\mathrm{F}}$ data in the large w limit we determine the quantity:

$$P = \alpha + \beta, \quad \text{where } \alpha = \frac{f_\downarrow T_{o\downarrow}}{f_\uparrow T_{o\uparrow}} \qquad \beta = \frac{T^*_{i\downarrow} T^*_{o\downarrow}}{T^*_{i\uparrow} T^*_{o\uparrow}}. \quad (3)$$

The term α is the ratio of minority to majority electrons emerging out of the first Co layer as $w \to 0$, and β is the ratio of the net transmission probabilities of the second Co layer. From these intercepts we find $P = 1.77$.

As noted, I_c does not substantially change whether a given Co thickness is composed of one or two layers. The transmission factors into and out of the second Co layer must, therefore, be close to unity, and β close to 1. We, therefore, set the transmission factors of the second Co layer to unity. With the value of α determined, we can now fit Eq. (1) to the $I_{c,\mathrm{F}}$ data using only three parameters ($\lambda_\uparrow$, $\lambda_\downarrow$, and an overall scale factor). The result is $\lambda_\uparrow = 21 \pm 1$ Å and $\lambda_\downarrow = 8.3 \pm 0.8$ Å, from which $\lambda_+ = 5.9$ Å is calculated, in good agreement with the result from the $I_{c,\mathrm{AF}}$ data. We note that the $w = 0$ intercept of this double-exponential fit is nearly identical (within 5%) to that of the single-exponential fit to the $I_{c,\mathrm{AF}}$ data, consistent with the transmission probabilities of the second Co layer being close to unity. These values for $\lambda_\uparrow$ and $\lambda_\downarrow$ are much smaller than the hot electron attenuation lengths found in free electron metals [9]. They are, however, larger than those previously reported [4] for higher energy (~5–10 eV) electrons in Co, consistent with the general expectation of an increase in attenuation length as the electron energy is decreased in the hot-electron regime.

To further test the model and results, the magnetic contrast $C = I_{c,\mathrm{F}}/I_{c,\mathrm{AF}}$, was measured and analyzed for a set of Co/Cu/Co trilayer samples with a 2:1 Co layer thickness ratio. For such samples

$$C = \frac{\alpha\beta \exp[-(w_1 + w_2)/\lambda_-] + 1}{\alpha \exp(-w_1/\lambda_-) + \beta \exp(-w_2/\lambda_-)}, \quad (4)$$

where $w_{1,2}$ is the thickness of the first (second) Co layer and $1/\lambda_- = 1/\lambda_\downarrow - 1/\lambda_\uparrow$. A least squares fit of Eq. (4), shown in Fig. 2(b), yields $\lambda_- = 13.3 \pm 0.5$ Å, using $\beta = 1$ and the previously determined value of $\alpha = 0.77$. We obtain $\lambda_- = 13.7 \pm 0.5$ Å from the fit of Eq. (4) to the 1:1 data, showing quite good agreement between the different measurements.

To investigate ballistic transport in this system at different energies, averaged $I_c - V_t$ data were taken at numerous positions of F and AF alignment in trilayer samples of varying Co thickness. In Fig. 3(a) we show the values of

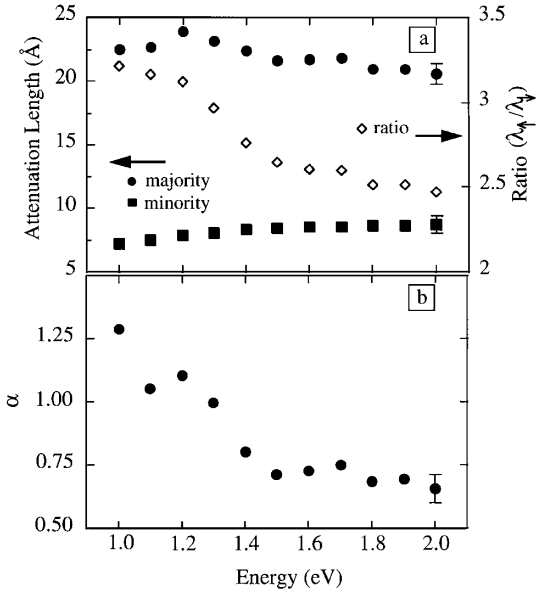

FIG. 3. (a) The attenuation lengths for majority and minority electrons and their ratio as a function of electron energy (injection bias). (b) Ratio of spin-down to spin-up electrons passing through the first Co/Cu interface (in the limit of zero Co thickness) as a function of energy.

$\lambda_\uparrow$ and $\lambda_\downarrow$ that we obtain from this data, using the model and method described above. Beginning at 1.0 eV, $\lambda_\downarrow$ is found to slightly increase up to $\sim$1.3 eV, above which it remains relatively constant. The top of the d-band contribution to the minority electron DOS is $\sim$1.3 eV above the Fermi energy, E_f. Thus we attribute the behavior of $\lambda_\downarrow$ to a crossover from the minority electrons propagating in the more localized d-band to propagating in the higher-velocity s-p band at increased energies [13]. $\lambda_\uparrow$ remains relatively constant up to $\sim$1.3 eV and then decreases slowly out to 2.0 eV. We tentatively attribute the behavior of $\lambda_\uparrow$ to the excitation of electrons in the majority d-band [14]. If at energies below $\sim$1.3 eV, the scattering is dominated by the excitation of electrons lying in the large peak in the DOS between $\sim$0.6 and 1.1 eV below E_f, then, as the number of filled states from which the hot electrons can excite electrons does not change substantially with energy, the attenuation length remains roughly constant. At energies above $\sim$1.3 eV, the electrons in the lower part of the d-band begin to significantly contribute to the hot-electron scattering, resulting in a slow decrease in $\lambda_\uparrow$ out to 2.0 eV. These combined effects lead to a rather large change in the ratio of the attenuation lengths between 1.2 and 1.3 eV.

From these same data, we also determine the energy dependence of α, the measure of the spin-dependent tunneling, and transmission across the first Co/Cu interface in the same manner described above for the 1.5 eV data. As we show in Fig. 3(b), above $\sim$1.3 eV, α remains relatively constant. As the energy is lowered, however, α begins to increase and continues to do so to the lowest energies accessible. This change in α also coincides with the large DOS change for minority electrons due to the d-band contribution. At energies below $\sim$1.2 eV, $\alpha > 1$ indicating that the net effect of spin-dependent tunneling to the Co surface and spin-dependent momentum filtering at the Co/Cu interface favors transport of minority spins out of the first Co layer, if it is very thin. Above $\sim$1.4 eV the hot electron current is weakly polarized in the opposite sense. As the Co layer becomes thicker than $\lambda_\downarrow$, however, the hot electron current becomes more and more strongly majority-spin polarized over the 1.0 to 2.0 eV energy range, due to the large difference in $\lambda_\uparrow$ and $\lambda_\downarrow$.

We thank A. C. Perrella, J. A. Katine, and D. C. Ralph for useful discussions and assistance and M. Stiles for a helpful communication. This research was supported by DARPA through ONR, and by the NSF through the Cornell Center for Materials Research and through use of the National Nanofabrication Users Network.

[1] D. J. Monsma, R. Vlutters, and J. C. Lodder, Science **281**, 407 (1998); D. J. Monsma, J. C. Lodder, Th. J. A. Popma, and B. Dieny, Phys. Rev. Lett. **74**, 5260 (1995).
[2] K. Mizushima, T. Kinno, K. Tanaka, and T. Yamauchi, Phys. Rev. B **58**, 4660 (1998).
[3] A. Filipe *et al.*, Phys. Rev. Lett. **80**, 2425 (1998); D. Oberli *et al.*, Phys. Rev. Lett. **81**, 4228 (1998); Y. U. Idzerda *et al.*, J. Appl. Phys. **64**, 5921 (1988).
[4] E. Vescovo *et al.*, Phys. Rev. B **52**, 13 497 (1995); D. P. Pappas *et al.*, Phys. Rev. Lett. **66**, 504 (1991); M. Getzlaff, J. Bansmann, and G. Schonhense, Solid State Commun. **87**, 467 (1993).
[5] M. Aeschlimann *et al.*, Phys. Rev. Lett. **79**, 5158 (1997).
[6] W. H. Rippard and R. A. Buhrman, Appl. Phys. Lett. **75**, 1001 (1999).
[7] W. J. Kaiser and L. D. Bell, Phys. Rev. Lett. **60**, 1406 (1988); L. D. Bell, W. J. Kaiser, M. H. Hecht, and L. C. Davis, in *Scanning Tunneling Microscopy*, edited by J. A. Stroscio and W. J. Kaiser (Academic Press, San Diego, 1993), p. 307.
[8] M. Prietsch, Phys. Rep. **253**, 163 (1995), and references therein.
[9] M. K. Weilmeier, W. H. Rippard, and R. A. Buhrman, Phys. Rev. B **59**, R2521 (1999).
[10] S. S. P. Parkin, R. Bhadra, and K. P. Roche, Phys. Rev. Lett. **66**, 2151 (1991).
[11] M. D. Stiles, J. Appl. Phys. **79**, 5805 (1996).
[12] N. F. Mott, Adv. Phys. **13**, 325 (1964).
[13] E. Yu. Tsymbal and D. G. Pettifor, Phys. Rev. B **54**, 15 314 (1996).
[14] E. Zarate, P. Apell, and P. M. Echenique, Phys. Rev. B **60**, 2326 (1999).